DOI 10.1007/s11182-020-01898-8

Russian Physics Journal, Vol. 62, No. 9, January, 2020 (Russian Original No. 9, September, 2019)

STATISTICAL ANALYSIS OF THE POTENTIAL OF A BATHYMETRIC LIDAR WITH TIME-OF-FLIGHT MATRIX SPAD PHOTODETECTOR

A. I. Potekaev,[1,2] A. A. Lisenko,[3] and V. S. Shamanaev[3]

UDC 551.46.07

The Monte Carlo method is used to solve the nonstationary laser sensing equation for a multicomponent optically dense water medium taking into account the influence of the water-air interface and the contributions of multiple radiation scattering by sea water and of the signal reflection from the sea bottom. Dependences of the signal power recorded with a monostatic lidar equipped with a time-of-flight matrix single-photon avalanche diode (SPAD) photodetector on the water depth and surface microwaves for different field-of-view angles of the receiver are obtained. Results of investigations have shown that the maximum depth of sea bottom detection is 40–50 m given that the optical water thickness does not exceed 3.5–4 m. The dynamic range of lidar signals from water reaches 7–9 orders of magnitude for lidar sensing of sea bottom at limiting depths of 40–50 m in very transparent water in the presence of the Fresnel reflection from the water surface. Results of statistical simulation have shown that the lidar system with the matrix receiver intended for sea water sensing can be realized at the modern technical level. Under favorable conditions, the lidar return signal power provides sensing of sea bottom to depths of 40–50 m.

Keywords: lidar, ocean optics, multiple radiation scattering, depth of sea bottom.

INTRODUCTION

Results of lidar measurements of sea water depths [1–3] have revealed physical and technical problems of signal recording and interpretation, primarily due to high water turbidity [4, 5] and necessity of high time resolution [6, 7]. The wavelength range of nanosecond pulsed lasers used for sea water sensing is physically limited by the blue-green region of the spectrum. Special attention should also be given to the Fresnel reflection of laser radiation from the air-water interface and multiple radiation scattering. Moreover, it was shown both theoretically and experimentally that the optical thickness τ from the sea water surface to the sea bottom should not exceed $\tau = 3.75–4.0$ [5]. This restriction is due to a large dynamic range of lidar return signal [5].

The available analytical approaches to a solution of the radiative transfer equation do not provide a detailed pattern of formation of received laser radiation considering all factors indicated above. The only opportunity of taking into account the complex of factors that influence the radiation interaction with the scattering and reflecting medium is the statistical approach to the solution of the radiative transfer equation [5].

In the present work, the dependences of the monostatic lidar return signal powers on the water depths are investigated as functions of the field-of-view angle of the lidar receiver. The nonstationary equation of laser radiation

[1]V. D. Kuznetsov Siberian Physical-Technical Institute at National Research Tomsk State University, Tomsk, Russia; [2]National Research Tomsk State University, Tomsk, Russia, e-mail: potekaev@spti.tsu.ru; [3]V. E. Zuev Institute of Atmospheric Optics of the Siberian Branch of the Russian Academy of Sciences, Tomsk, Russia, e-mail: lisenko@iao.ru; shvs@iao.ru. Translated from Izvestiya Vysshikh Uchebnykh Zavedenii, Fizika, No. 9, pp. 165–170, September, 2019. Original article submitted June 8, 2019.

propagation in sea water is solved by the Monte Carlo method taking into account the effect of the air-water interface, the contribution of multiple laser radiation scattering, and the Lambert reflection of lidar signals from the sea bottom.

APPROACH TO THE PROBLEM SOLUTION, MODEL OF THE PROPAGATION MEDIUM, AND GEOMETRY OF THE EXAMINED PROBLEM

Let us consider a monostatic pulsed range-gated laser sensing system placed onboard an aircraft flying with velocity V at altitude H above the sea water surface intended for sea water sensing. Laser radiation is propagated in the nadir, passed through the air-water interface, absorbed and scattered in water, reflected from the sea bottom, intersected the water-air interface, and recorded with a detector. The atmospheric conditions are disregarded. The distance from the lidar to the sea bottom is the sum of the aircraft flight altitude H and the depth h in the sea water (disregarding its refractive index). The laser radiation reflection coefficient from the sea bottom is ρ. The lidar return signal in this case is determined by backscattering on hydrosol particles, molecular scattering by water, and multiple scattering by water. Along with the useful signal, the background noise signal caused by atmospheric optical radiation in the passband of the detector (including radiation of the Sun, the Moon, and the sky) is also recorded by a matrix photodetector.

In laser sensing of scattering media, the useful signal that carries information is the signal of single scattering in the direction toward the optical detector is described mathematically by the canonical equation

$$P_0(h) = W_0 A \sigma_\pi(h) h^{-2} \exp\left\{-2\int_0^h \sigma(h)\,dh\right\}, \tag{1}$$

where $P_0(h)$ is the recorded signal, W_0 is the energy of the sensing laser pulse, A is the instrumental function, and $\sigma_\pi(h)$ and $\sigma(h)$ are the volume backscattering and extinction coefficients.

The lidar return signal power $P(h)$ is the sum of the following additive components:

$$P(h) = P_0(h) + P_\mathrm{b}(h) + P_{0\,\mathrm{m}}(h),$$

where $P_0(h)$ is the signal of single scattering on aerosol and hydrosol particles and of molecular scattering by pure water, $P_\mathrm{b}(h)$ is the multiply scattered background signal, and $P_{0\,\mathrm{m}}(h)$ is the signal component reflected by the water surface.

Let us consider the total noise background radiation. The background signal power P_b for the detector with a narrow field-of-view angle and narrow-band optical interference filter is

$$P_\mathrm{b} = L_\mathrm{b} \Delta\lambda \pi r_r^2 \Omega_r, \tag{2}$$

where L_b is the spectral brightness of side illumination, $\Delta\lambda$ is the width of the filter passband, $\Omega_r = \pi\alpha_r^2$ is the instantaneous current solid field-of-view angle of the detector, and r_r is the radius of the receiving aperture. For a lidar operating through the air-water interface, the brightness of side illumination L_b recorded with the detector of the lidar located at altitude H above the water surface for observation in the nadir is

$$L_f = L_h + L_s + L_{sf}.$$

Here L_h is the brightness of the atmospheric haze (brightness of light scattered by the underlying atmosphere layer directly toward the receiver), L_s is the brightness of radiation emerging from water, and L_{sf} is the brightness of

radiation reflected from the water surface. The brightness components L_h, L_s, and L_{sf} are determined from the following formulas:

$$L_h = \frac{\pi S_\lambda \cos\theta_0}{4\pi(1+\cos\theta_0)} \exp(\tau_0 - \tau)$$

$$\times \left\{ \exp\left[-(\tau_0 - \tau)\left(1 + \frac{1}{\cos\theta_0}\right)\right] - \exp\left[-\left(\tau_0\left(1 + \frac{1}{\cos\theta_0}\right)\right)\right]\right\}; \quad (3)$$

$$L_s = T_{sf}^{\downarrow} \frac{T_{sf}^{\uparrow}}{m^2} E \rho_s \exp(-\tau), \quad (4)$$

$$L_{sf} = T_{sf}^{\downarrow} \frac{\rho_{sf} E}{\pi} \exp(-\tau). \quad (5)$$

Here E is the side illumination of the water surface by the Sun and sky:

$$E = 2\frac{1 + \frac{3}{2}\mu_0 + \left(1 - \frac{3}{2}\mu_0\right)\exp\left[\frac{-\tau_0}{\mu_0}\right]}{\left[4 + (3 - x_1)\tau_0\right]} E_0, \quad (6)$$

where $\mu_0 = \cos\theta_0$ is the cosine of the solar zenith angle θ_0, τ_0 is the optical thickness of the atmosphere, x_1 is the parameter of the scattering phase function of the atmosphere (the first term of the expansion in the Legendre polynomial), $E_0 = E_\perp \mu_0$ is the illumination at the upper boundary of the atmosphere, $E_\perp$ is the spectral solar constant, $T_{sf}^{\downarrow}$ is the sea surface transmission coefficient for solar radiation incident from the atmosphere, $T_{sf}^{\uparrow}$ is the sea surface transmission coefficient for solar radiation emitting from water, m is the water refractive index, ρ_s is the brightness coefficient depending on the water type, ρ_{sf} is the brightness coefficient of the water surface depending on the solar zenith angle θ_0 and the wind speed U, and $\tau = \varepsilon H$ is the optical thickness of the atmospheric layer from the water surface to the lidar.

In case of sensing the sea bottom from small flight altitudes, it is possible to take $L_h \cong 0$ and $\exp(-\tau) \cong 1$; then for the brightness of radiation arriving at the lidar detector L_b, we obtain

$$L_b \cong \left(\frac{T_{sf}^{\downarrow} T_{sf}^{\uparrow}}{m^2} \rho_s + \frac{\rho_{sf}}{\pi} \right) E. \quad (7)$$

For another limiting case of sensing the sea bottom from high flight altitudes ($H \geq 10$ km), we obtain

$$L_b \cong \frac{E_\perp \cos\theta_0}{4\pi(1+\cos\theta_0)} \left\{ 1 - \exp\left[-\tau_0\left(1 + \frac{1}{\cos\theta_0}\right)\right]\right\} + \left(\frac{T_{sf}^{\downarrow} T_{sf}^{\uparrow}}{m^2} \rho_s + \frac{\rho_{sf}}{\pi} \right) E. \quad (8)$$

STATISTICAL ESTIMATES OF THE SIGNAL/NOISE RATIO BY THE PHOTON COUNTING METHOD

The discrete nature of background noise signals, for example, shot noise of the detector can have considerable effect when the noise level is reduced or the useful signal duration is decreased. Therefore, along with the methods of optical signal reception and transformation into the electric signal, the dynamic operation mode is used in which single current or voltage pulses are recorded. Sometimes it is called the photon counting method or the method of counting single-electron pulses. In the dynamic method, the output signal of the receiver is characterized by the rate of counting of pulses from separate light quanta hitting the photosensitive layer. The average number of photoelectrons produced by the light flux P_s hitting the detector is

$$\overline{n}_s = \frac{\eta P_s}{h\nu}, \tag{9}$$

where η is the quantum efficiency of the photodetector, ν is the optical radiation frequency, and h is Planck's constant.

If a photoelectron multiplier (PEM) is used as a detector, each photoelectron induces an electron avalanche on the anode that charges its distributed output capacitance. Adjusting the threshold level of electron circuit triggering, it is possible to suppress a considerable part of background noise pulses arising out of the photocathode.

If all pulses have been time-resolved, the probability of occurrence of n pulses per unit time is described by the Poisson law (the number n fluctuates about $\overline{n}_{av}$):

$$\omega(n, \overline{n}_{av}) = (\overline{n}_{av})^n \exp(-\overline{n}_{av}) / n!. \tag{10}$$

Thus, the signal/noise ratio is

$$SNR = \frac{(\overline{n}_{av}\tau_g)^2}{\left[\sqrt{(\overline{n}_{av} + \overline{n}_b + \overline{n}_n)\tau_g}\right]^2} = \frac{\overline{n}_{av}^2 \tau_g}{\overline{n}_{av} + \overline{n}_b + \overline{n}_n}, \tag{11}$$

where τ_g is the measurement time (gating period), $\overline{n}_n$ is the average number of photoelectrons generated by internal noise, and $\overline{n}_b$ is the average number of external background photoelectrons. In order that the number of electrons $\overline{n}_{av}$ exceeded the threshold number n_L, the probability of triggering should be

$$\omega(n \geq n_L, \overline{n}_s) = \sum_{n=n_L}^{\infty} \left[(\overline{n}_s)^n \exp(-\overline{n}_s) / n! \right]. \tag{12}$$

From the last expression, we can estimate the number of electrons $\overline{n}_{av\min}$ corresponding to the probability $\omega(n, \overline{n}_s)$.

The advantage of this method is that the entire signal energy is used for pulse counting, whereas in the direct and heterodyne methods, a part of signal energy is lost. Discrete recording of each pulse allows the effect of background noise caused by the application of the multiplication system of the photodetector to be reduced.

RESULTS AND DISCUSSION

To solve the nonstationary radiative transfer equation, the initial optical characteristics of sea water should be assigned, including the absorption index a, the scattering index b, the extinction coefficient $c = a + b$, and the photon survival probability $w = b/c$ together with the scattering phase function describing the dependence of the scattered radiation intensity on the angle φ between the incident and scattered beams.

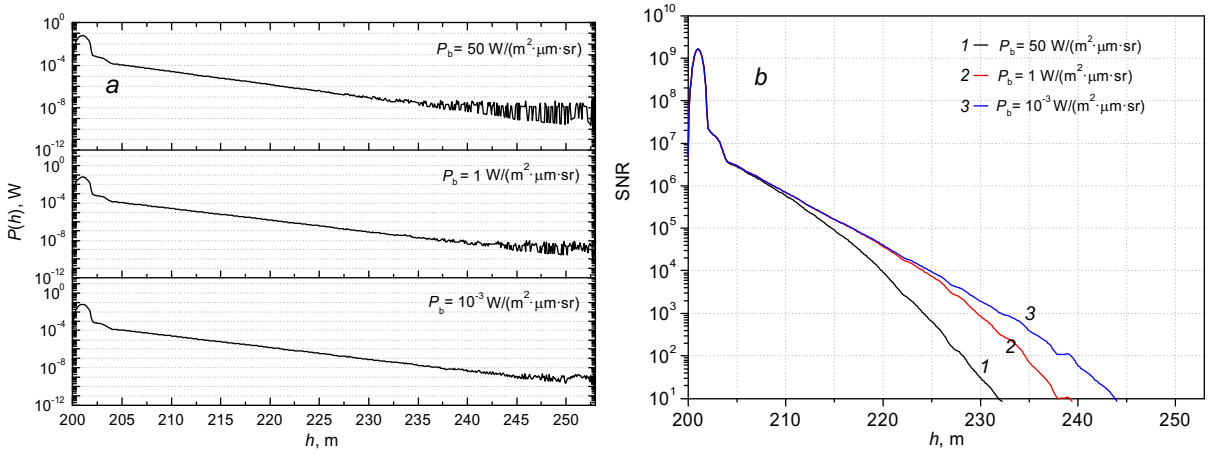

Fig. 1. Dependences of the total signal power $P(h)$ recorded by the matrix photodetector including signal components scattered in water and reflected from the water surface and bottom (*a*) and of the signal/noise ratio (*b*) on the water depth h for pure ocean water with the P2 scattering phase function for $a = 0.114$ m^{-1}, $b = 0.037$ m^{-1}, $c = 0.151$ m^{-1}, and $w = 0.245$. Values of the background side illumination brightness are indicated near the curves.

The range of variations of the hydrooptical characteristics of ocean water is very large: 2–3 orders of magnitude depending on its chemical and physical composition. Disregarding the effect of air bubbles in the subsurface water layer, its hydro-optical properties are determined by three optically active components: pure water, dissolved biological matter, and hydrosol suspension. The optical characteristics of water can be represented as the sum of the following components:

$$\sigma_\Sigma = \sigma_{SW} + \sigma_{AW} + \sigma_{SP} + C_{ch}\alpha_{ch} + C_y\alpha_y,$$

where σ_{SW} and σ_{AW} are the scattering and absorption indices of pure water, σ_{SP} is the scattering index of particles suspended in water, and C_{ch}, C_y, α_{ch}, and α_y are the concentrations and the specific absorption indices of chlorophyll and yellow substance (dissolved organic matter). Molecular scattering of laser radiation by water obeys the Rayleigh law and is practically identical for all waters of the World Ocean.

The scattering phase function is a very important optical parameter that characterizes the scattering particles and determines laser radiation propagation in the turbid medium. The low-parameter models of the scattering phase functions P0–P15 proposed by Petzold [6] are often used for calculations. Figures 1–3 show the calculated lidar return signals for the sea water scattering phase functions of three types according to the Petzold classification: P2 for pure ocean water (Fig. 1), P5 for ocean water in the coastal zone (Fig. 2), and P7 for turbid water in a harbor (Fig. 3).

From the results shown in Figs. 1–3 it can be seen that at night ($P_b = 10^{-3}$ W/(m^2·μm·sr)) the signal/noise ratio for pure ocean water exceeds 10 up to depths of 44 m, up to depth of 24 m for ocean water in coastal zone, and up to depth of 12 m for turbid water. This confirms the feasibility of reliable signal detection with the matrix photodetector up to these depths.

In this case, the optical scanning system with high scanning rate is not required due to the use of the time-of-flight matrix photodetector. Its rectangular field-of-view moves along the aircraft (helicopter) flight direction with a relatively low velocity. The total image of the investigated water volume is obtained by *sewing together* the moving rectangular images (lidar shots). In this case, each pixel displays the distance from lidar, and the entire pattern provides the 3D image of water with the sea bottom.

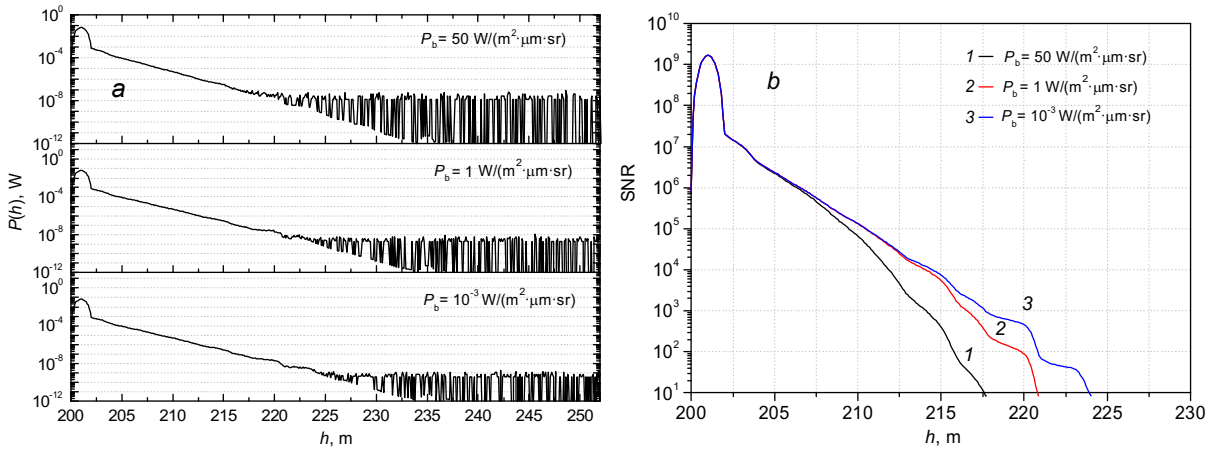

Fig. 2. Dependences of the total signal power $P(h)$ recorded by the matrix photodetector including signal components scattered in water and reflected from its surface and bottom on the water depth h (*a*) and of the signal/noise ratio (*b*) for ocean water in the coastal zone with the P5 scattering phase function for $a = 0.114$ m^{-1}, $b = 0.037$ m^{-1}, $c = 0.151$ m^{-1}, and $w = 0.245$. Values of the background side illumination brightness are indicated near the curves.

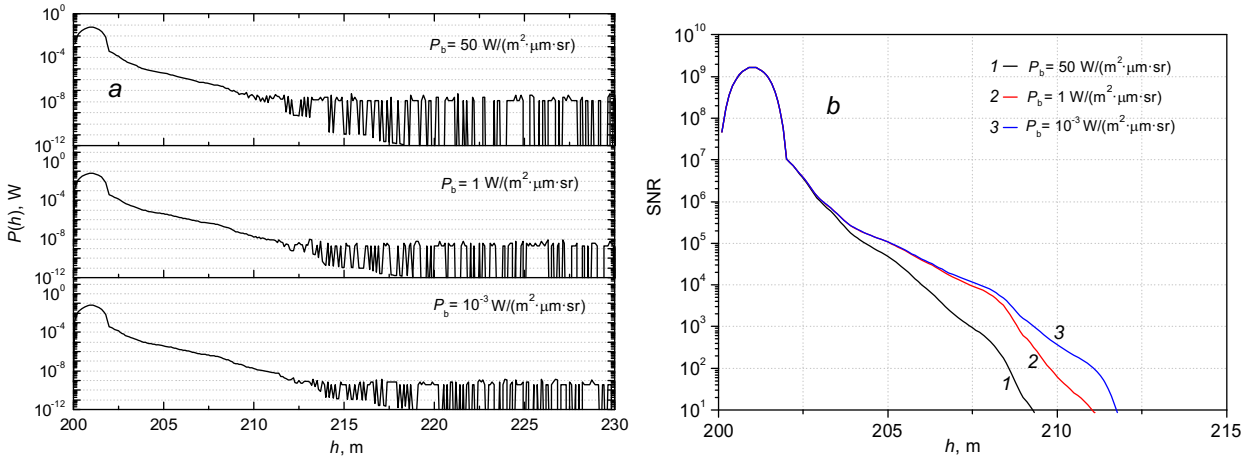

Fig. 3. Dependences of the total signal power $P(h)$ recorded by the matrix photodetector including signal components scattered in water and reflected from its surface and bottom (*a*) and of the signal/noise ratio (*b*) depending on the water depth for turbid water in a harbor with the P5 scattering phase function for $a = 0.366$ m^{-1}, $b = 1.824$ m^{-1}, $c = 2.19$ m^{-1}, and $w = 0.833$. Values of background side illumination brightness are indicated near the curves.

CONCLUSIONS

Results of statistical simulation have shown that the lidar system of sea water sensing with the matrix detector can be successfully realized. The power of signals recorded with the matrix photodetector under favorable conditions provides reliable water sensing to depths of 44 m.

The nonstationary laser sensing equation has been solved by the Monte Carlo method for a multi-component water medium taking into account the air-water interface and the contribution of multiple laser radiation scattering by sea water and signal reflected from the sea bottom. The dependences of the monostatic lidar return signal powers recorded with the matrix photodetector of the lidar placed onboard a flying vehicle on the water depth and wind-driven sea waves have been obtained for various detector field-of-views. Results of our investigations have shown that the maximum depth of lidar detection of sea bottom is 40–50 m for optical water thickness of 3.5–4. In sensing of the limiting depth of the sea bottom for very transparent water in the presence of the Fresnel signal reflection from the water surface, the dynamic range of lidar return signals reaches 7–9 orders of magnitude.

Results of statistical simulation have shown that the lidar system of sea water sensing with the matrix detector can be realized at the modern technical level. The powers of signals of this lidar under favorable conditions allow lidar sensing of ocean waters to be performed to depths of 40–50 m.

REFERENCES

1. K. J. Lee, Y. Park, A. Bunkin, *et al*., Appl. Opt., **41**, No. 3, 401–406 (2000).
2. K. Fredriksson, B. Galle, K. Nystrom, *et al*., Underwater laser-radar experiments for bathymetry and fish school detection, Report GJPR-162, Goteborg Inst. Phys. (1978).
3. V. S. Shamanaev, I. E. Penner, G. P. Kokhanenko, and M. M. Krekova, Nauka-Proizv., No. 9 (65), 20–23 (2003).
4. V. A. Gladkikh, V. G. Lizogub, G. P. Kokhanenko, and V. S. Shamanaev, Prib. Tekh. Eksp., No. 1, 85–88 (1996).
5. V. S. Shamanaev, A. I. Potekaev, A. A. Lisenko, and M. G. Krekov, Russ. Phys. J., **59**, No. 12, 2034–2040 (2016).
6. T. J. Petzold, Volume scattering functions for selected ocean waters, SIO Ref. 72–78, Scripps Institute of Oceanography, Visibility Laboratory, San Diego (1972).